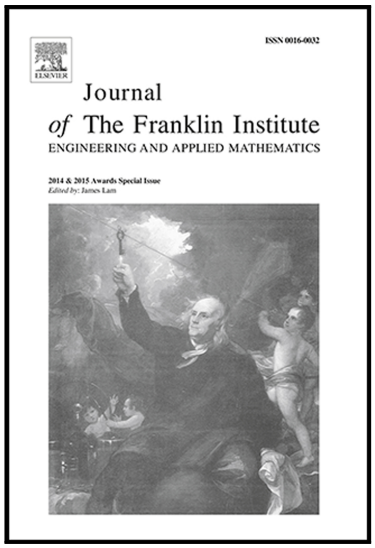

Proposing, developing and verification of a novel discrete-time zeroing neural network for solving future augmented Sylvester matrix equation

Yang Shi, Long Jin, Shuai Li, Jipeng Qiang

PII: S0016-0032(20)30108-3
DOI: https://doi.org/10.1016/j.jfranklin.2020.02.024
Reference: FI 4436

To appear in: *Journal of the Franklin Institute*

Received date: 25 May 2019
Revised date: 12 December 2019
Accepted date: 18 February 2020

Please cite this article as: Yang Shi, Long Jin, Shuai Li, Jipeng Qiang, Proposing, developing and verification of a novel discrete-time zeroing neural network for solving future augmented Sylvester matrix equation, *Journal of the Franklin Institute* (2020), doi: https://doi.org/10.1016/j.jfranklin.2020.02.024

Proposing, developing and verification of a novel discrete-time zeroing neural network for solving future augmented Sylvester matrix equation ☆

Yang Shi[a,*], Long Jin[b], Shuai Li[c], Jipeng Qiang[a]

[a] *School of Information Engineering, Yangzhou University, Yangzhou 225127, China*
[b] *School of Information Science and Engineering, Lanzhou University, Lanzhou 730000, China*
[c] *College of Engineering, Swansea University, Swansea, U.K.*

Abstract

In this paper, a novel discrete-time advance zeroing neural network (DT-AZNN) model is proposed, developed and investigated for solving future augmented Sylvester matrix equation (F-ASME). First of all, based on the advance zeroing neural network (AZNN) design formula, a novel continuous-time advance zeroing neural network (CT-AZNN) model is shown for solving continuous-time augmented Sylvester matrix equation (CT-ASME). Secondly, a recently published discretization formula is further investigated with the optimal sampling gap of the discretization formula proposed. Then, for solving F-ASME, a novel DT-AZNN model is proposed based on the discretization formula. Theoretical analyses on the convergence property and the perturbation suppression performance of the DT-AZNN model are provided. Moreover, comparative numerical experimental results are conducted to prove the effectiveness and robustness of the proposed DT-AZNN model for solving F-ASME.

Keywords: Future augmented Sylvester matrix equation, Zeroing neural network, Discretization formula, Robustness

☆This work is supported by the National Natural Science Foundation of China (with numbers 61906164, 61703189 and 61703362) and by the Natural Science Foundation of Jiangsu Province of China (with numbers BK20190875 and BK20170513).

*Corresponding author.
E-mail Addresses: shiy@yzu.edu.cn, shiyang0830@gmail.com

1. Introduction

As one of the fundamental mathematical problems, Sylvester matrix equation is widely encountered in scientific and engineering fields [1, 2, 3, 4, 5], the general form of which is formulated as

$$AX + XB = C \in \mathbb{R}^{m\times n},$$

where $A \in \mathbb{R}^{m\times m}$, $B \in \mathbb{R}^{n\times n}$ and $C \in \mathbb{R}^{m\times n}$ are the known matrices; $X \in \mathbb{R}^{m\times n}$ is the unknown matrix to be solved. For example, as a special case of Sylvester matrix equation, Lyapunov matrix equation is broadly used to analyze the stability of dynamic systems [6]. There exist a great number of mathematical methods, e.g., the Bartels-Stewart algorithm [7] and its extensions [8, 9], which is equipped with a time complexity $O(n^3)$ [9], for effectively solving Sylvester matrix equation. However, on the one hand, lots of methods are essentially designed for solving time-invariant (or say, static) Sylvester matrix equation rather than time-variant Sylvester matrix equation. In this sense, these methods do not possess enough efficiency for handing nonstationary cases due to the lack of adaption to the time-variant parameters [10]. On the other hand, few researches on investigating the discrete-time Sylvester matrix equation compared with the continuous-time one [9, 11, 12, 13, 14, 15, 16, 17]. With the development of digital circuits and digital computers, the discrete-time problem fits well with the actual applications, and the discrete-time models are more convenient for numerical implementation on digital systems. Thus, it is important to investigate the discrete-time Sylvester matrix equation.

Neural networks, especially recurrent neural networks, have been widely utilized for solving various problems in the past decades [18, 19, 20, 21, 22, 23, 24]. A novel recurrent neural network is proposed by Zhang et al. for solving Sylvester matrix equation with time-variant coefficient matrices for the first time [11]. Such type of recurrent neural network aims at zeroing indefinite error function for a specific problem, and is thus called zeroing neural network (ZNN) [18, 25, 26, 27, 28]. Based on the previous researches, the continuous-time classical zeroing neural network (CT-CZNN) model can accurately obtain a solution of continuous-time Sylvester matrix equation [11]. However, most of these researches are considered under ideal conditions. In fact, in the practical applications, perturbations always exist and have significant influence on the solving system process. Jin et al. firstly proposed

continuous-time advance zeroing neural network (CT-AZNN) models for solving perturbed continuous-time problems [29, 30]. As further researches, the discrete-time advance zeroing neural network (DT-AZNN) model is verified to possess excellent performance in the presence of perturbations [31, 32].

Together with previous researches, in this paper, a novel DT-AZNN model is utilized to solve the future augmented Sylvester matrix equation (F-ASME), which originates from the continuous-time augmented Sylvester matrix equation (CT-ASME). Specifically, on the one hand, the augmented Sylvester matrix equation (ASME) can be formulated as

$$AXB + CXD = E \in \mathbb{R}^{m\times n},$$

where $A \in \mathbb{R}^{m\times m}$, $B \in \mathbb{R}^{n\times n}$, $C \in \mathbb{R}^{m\times m}$, $D \in \mathbb{R}^{n\times n}$ and $E \in \mathbb{R}^{m\times n}$ are the known matrices; $X \in \mathbb{R}^{m\times n}$ is the unknown matrix to be calculated. Evidently, the above matrix equation includes the well-known Lyapunov matrix equation, Stein matrix equation and Sylvester matrix equation [33, 34], which means that the Lyapunov matrix equation, Stein matrix equation and Sylvester matrix equation can be regarded as special cases of ASME. On the other hand, the future problem is a special discrete-time problem. During the solving process, based on the present and/or previous data, we compute the results for future use before the next time instant [32]. That is, for solving future problems, an effective method should not only obtain the solution of discrete-time problems, but also should satisfy the requirement of real-time computation.

The remainder of this paper is organized into five sections. In Section 2, the problem formulation is described, and then the problem transformation and corresponding continuous-time models are presented. In Section 3, a recently published discretization formula is further studied, and we further propose corresponding DT-AZNN model. Theoretical analyses of such model are also proposed in this section. Section 4 shows comparative numerical experiments to substantiate the effectiveness and robustness of the proposed DT-AZNN model. Section 5 concludes this paper with final remarks. Before ending this section, it is worth pointing out the main contributions of this paper as follows.

1) In this paper, aided with the Kronecker product and vectorization techniques, the CT-ASME is transformed into a simple continuous-time linear system, which is further solved by the proposed CT-AZNN model with superior perturbation suppression performance.

2) Based on the previous researches, a recently published one-step-ahead discretization formula (termed 5-instant discretization formula) is presented for further investigation. As an important property of the discretization formula, in this paper, the optimal sampling gap of the 5-instant discretization formula is proposed and proved firstly, which can be seen as a mathematical breakthrough in the research front of the discretization formula.

3) By using the above discretization formula to discretize CT-AZNN model, a novel DT-AZNN model is proposed, developed and investigated for solving F-ASME with corresponding theoretical analyses presented to show its convergence property and perturbation suppression performance.

4) Comparative numerical experiments are conducted to substantiate the effectiveness and robustness of the proposed DT-AZNN model in the presence of various perturbations (including the constant perturbation, the linear-form time-variant perturbation, the sine-form/cosine-form time-variant perturbation and the exponential-decay-form time-variant perturbation).

In addition, the list of acronyms is summarized as below.

Acronyms

ASME: Augmented Sylvester matrix equation.
AZNN: Advance zeroing neural network.
CZNN: Classical zeroing neural network.
CT-AZNN: Continuous-time advance zeroing neural network.
CT-ASME: Continuous-time augmented Sylvester matrix equation.
CT-CZNN: Continuous-time classical zeroing neural network.
DT-AZNN: Discrete-time advance zeroing neural network.
DT-CZNN: Discrete-time classical zeroing neural network.
F-ASME: Future augmented Sylvester matrix equation.
ZNN: Zeroing neural network.

2. Problem formulation, problem transformation and continuous-time ZNN models

To lay a basis for further investigation, in this section, problem formulation is presented firstly. Then, the problem transformation and corresponding continuous-time ZNN models are also presented.

2.1. Problem formulation

First of all, let us consider the following F-ASME, which should be solved at time interval $[t_k, t_{k+1}) \subseteq [t_0, t_{\mathrm{f}}] \subseteq [0, +\infty)$, as

$$A_{k+1}X_{k+1}B_{k+1} + C_{k+1}X_{k+1}D_{k+1} - E_{k+1} = \mathbf{0} \in \mathbb{R}^{m\times n}, \tag{1}$$

where future coefficient matrices $A_{k+1} \in \mathbb{R}^{m\times m}$, $B_{k+1} \in \mathbb{R}^{n\times n}$, $C_{k+1} \in \mathbb{R}^{m\times m}$, $D_{k+1} \in \mathbb{R}^{n\times n}$ and $E_{k+1} \in \mathbb{R}^{m\times n}$ are defined to be generated from the smoothly continuous-form of time-variant matrices $A(t) \in \mathbb{R}^{m\times m}$, $B(t) \in \mathbb{R}^{n\times n}$, $C(t) \in \mathbb{R}^{m\times m}$, $D(t) \in \mathbb{R}^{n\times n}$ and $E(t) \in \mathbb{R}^{m\times n}$ by sampling at time instant $t = (k+1)g$ (termed t_{k+1}), respectively; $X_{k+1} \in \mathbb{R}^{m\times n}$ is the unknown matrix. In addition, $g > 0$ denotes the sampling gap, and $k = 0, 1, 2, \cdots$ denotes the updating index. As mentioned above, the ASME includes the well-known Lyapunov matrix equation, Stein matrix equation and Sylvester matrix equation [33, 34], which highlights again the mathematical significance and breakthrough of this paper. In addition, inspired by [31, 32], we mainly focus on solving future problem, which can be regarded as a special kind of discrete-time problem, and then the designed model should satisfy the requirement of future computation during the solution process. Specifically, at time instant t_k, the present and previous data (e.g., X_k, A_k, B_k and corresponding derivatives) are gainable, but the unknown data (e.g., X_{k+1} and corresponding derivative) have not been obtained yet. In other words, these data can not participate in the computation at time instant t_k [32].

2.2. ZNN design formulas

To obtain the solution to F-ASME (1), let us consider the following CT-ASME, which is evolved from (1):

$$A(t)X(t)B(t) + C(t)X(t)D(t) - E(t) = \mathbf{0} \in \mathbb{R}^{m\times n}, \tag{2}$$

with $t \in [0, t_{\mathrm{f}}] \subseteq [0, +\infty)$; continuous-form of time-variant matrices $A(t) \in \mathbb{R}^{m\times m}$, $B(t) \in \mathbb{R}^{n\times n}$, $C(t) \in \mathbb{R}^{m\times m}$, $D(t) \in \mathbb{R}^{n\times n}$ and $E(t) \in \mathbb{R}^{m\times n}$. To monitor and control (2), the time-variant zeroing error function can be defined

as

$$Z(t) = A(t)X(t)B(t) + C(t)X(t)D(t) - E(t). \tag{3}$$

Then, according to [11, 26], the CZNN design formula is selected for zeroing out $Z(t)$ such that the time-variant zeroing error function converges to zero exponentially [35]:

$$\dot{Z}(t) = -\gamma\phi(Z(t)),$$

where $\dot{Z}(t)$ denotes the time-derivative of $Z(t)$; the design parameter $\gamma > 0$ is used to scale the convergence rate; $\phi(\cdot) : \mathbb{R}^{m\times n} \to \mathbb{R}^{m\times n}$ denotes an activation function mapping array. For simplicity and clarity, applying the linear activation function array [36] to the above CZNN design formula leads to

$$\dot{Z}(t) = -\gamma Z(t). \tag{4}$$

Besides, the AZNN design formula has been recently presented for time-variant problems solving [31, 32, 37]. For the convenience of presentation and readability, the derivation process of AZNN design formula has been presented in [32], and is omitted due to the space limitation. The AZNN design formula is presented for zeroing $Z(t)$ as follows:

$$\dot{Z}(t) = -2\mu Z(t) - \mu^2 \int_0^t Z(\sigma)\mathrm{d}\sigma. \tag{5}$$

2.3. Problem transformation and continuous-time ZNN models

In this subsection, inspired by Kronecker product and vectorization techniques [38, 39], the CT-ASME (2) can be vectorized equivalently as

$$\mathrm{vec}(Z(t)) = \big(B^{\mathrm{T}}(t) \otimes A(t) + D^{\mathrm{T}}(t) \otimes C(t)\big)\,\mathrm{vec}(X(t)) - \mathrm{vec}(E(t))$$

with Kronecker product $\otimes$ and matrix vectorization operation $\mathrm{vec}(\cdot)$. In addition, the time derivative of $Z(t)$ can be presented as

$$\begin{aligned}\dot{Z}(t) =& \dot{A}(t)X(t)B(t) + A(t)\dot{X}(t)B(t) + A(t)X(t)\dot{B}(t) + \dot{C}(t)\\ & X(t)D(t) + C(t)\dot{X}(t)D(t) + C(t)X(t)\dot{D}(t) - \dot{E}(t),\end{aligned}$$

which can be vectorized equivalently as

$$\begin{aligned}\mathrm{vec}(\dot{Z}(t)) = &\Big(B^{\mathrm{T}}(t) \otimes \dot{A}(t) + \dot{B}^{\mathrm{T}}(t) \otimes A(t)\Big)\,\mathrm{vec}(X(t)) +\\ &\Big(D^{\mathrm{T}}(t) \otimes \dot{C}(t) + \dot{D}^{\mathrm{T}}(t) \otimes C(t)\Big)\,\mathrm{vec}(X(t)) +\\ &\big(B^{\mathrm{T}}(t) \otimes A(t) + D^{\mathrm{T}}(t) \otimes C(t)\big)\,\mathrm{vec}(\dot{X}(t)) - \mathrm{vec}(\dot{E}(t)).\end{aligned}$$

Define

$$\begin{cases} M(t) = B^{\mathrm{T}}(t) \otimes A(t) + D^{\mathrm{T}}(t) \otimes C(t) \\ \dot{M}(t) = B^{\mathrm{T}}(t) \otimes \dot{A}(t) + \dot{B}^{\mathrm{T}}(t) \otimes A(t) + D^{\mathrm{T}}(t) \otimes \dot{C}(t) + \dot{D}^{\mathrm{T}}(t) \otimes C(t). \end{cases}$$

Thus, we have

$$\dot{\mathbf{z}}(t) = \dot{M}(t)\mathbf{x}(t) + M(t)\dot{\mathbf{x}}(t) - \dot{\mathbf{e}}(t), \tag{6}$$

where $\dot{\mathbf{z}}(t)$, $\dot{\mathbf{x}}(t)$ and $\dot{\mathbf{e}}(t)$ denote the vectorization of $\dot{Z}(t)$, $\dot{X}(t)$ and $\dot{E}(t)$, respectively. Note that the above equation (6) is the time derivative of the following one:

$$\mathbf{z}(t) = M(t)\mathbf{x}(t) - \mathbf{e}(t), \tag{7}$$

which can be viewed as a standard continuous-time linear system [26]. It can be concluded that, based on the Kronecker product and vectorization techniques, the CT-ASME (2) can be transformed into a relatively simple continuous-time linear system. In other words, we present a link between the CT-ASME (2) and continuous-time linear system (7).

Combining the continuous-time linear system (7) with the AZNN design formula (5) generates the following CT-AZNN model:

$$\begin{aligned} M(t)\dot{\mathbf{x}}(t) = &- 2\mu\left(M(t)\mathbf{x}(t) - \mathbf{e}(t)\right) - \mu^2 \int_0^t \left(M(\sigma)\mathbf{x}(\sigma) - \mathbf{e}(\sigma)\right) \mathrm{d}\sigma \\ &- \dot{M}(t)\mathbf{x}(t) + \dot{\mathbf{e}}(t). \end{aligned} \tag{8}$$

Considering the effect of the perturbations in the solving process, the perturbed CT-AZNN model can be obtained as

$$\begin{aligned} M(t)\dot{\mathbf{x}}(t) = &- 2\mu\left(M(t)\mathbf{x}(t) - \mathbf{e}(t)\right) - \mu^2 \int_0^t \left(M(\sigma)\mathbf{x}(\sigma) - \mathbf{e}(\sigma)\right) \mathrm{d}\sigma \\ &- \dot{M}(t)\mathbf{x}(t) + \dot{\mathbf{e}}(t) + \mathbf{p}(t), \end{aligned} \tag{9}$$

of which $\mathbf{p}(t)$ signifies the measurement perturbations including the ambient perturbations and the hardware errors. For comparison, the CT-CZNN model based on the CZNN design formula (4) is presented as

$$M(t)\dot{\mathbf{x}}(t) = -2\mu\left(M(t)\mathbf{x}(t) - \mathbf{e}(t)\right) - \dot{M}(t)\mathbf{x}(t) + \dot{\mathbf{e}}(t). \tag{10}$$

Theorem 1. *Consider perturbed CT-AZNN model (9) with time-variant perturbation* $\mathbf{p}(t)$*. The Laplace transformation result of time-variant perturbation* $\mathbf{p}(t)$ *is defined as* $\mathbf{p}(s)$*. If* $\lim_{s\to 0} s^2\mathbf{p}(s)$ *exists, the perturbed CT-AZNN model (9) converges toward theoretical solution to CT-ASME (2) with corresponding residual error.*

Proof. Consider perturbed CT-AZNN model (9) with time-variant perturbation $\mathbf{p}(t)$. Using the Laplace transformation [40] to the jth subsystem of the perturbed CT-AZNN model (9) generates

$$z_j(s) = \frac{s(z_j(0) + p_j(s))}{s^2 + 2s\mu + \mu^2},$$

where $\mu > 0$. It can be concluded that the subsystem is stable [29, 30, 31]. For such a stable system, the final value theorem can be applied [30]. Hence, we have

$$\lim_{t\to\infty} z_j(t) = \lim_{s\to 0} sz_j(s) = \lim_{s\to 0} \frac{s^2(z_j(0) + p_j(s))}{s^2 + 2s\mu + \mu^2} = \lim_{s\to 0} \frac{s^2 z_j(0)}{(s+\mu)^2} + \lim_{s\to 0} \frac{s^2 p_j(s)}{(s+\mu)^2}.$$

Thereinto, $z_j(0)$ is a constant, and thus $\lim_{s\to 0} s^2 z_j(0)/(s+\mu)^2 = 0$. Moreover, it can be seen that if $\lim_{s\to 0} s^2 p_j(s)$ exists, $\lim_{s\to 0} sz_j(s)$ exists, and then $\lim_{t\to\infty} \|\mathbf{z}(t)\|_2$ exists. In this situation, the perturbed CT-AZNN model (9) converges toward theoretical solution to CT-ASME (2) with corresponding steady-state residual error. The proof is thus completed. □

Based on the Theorem 1, we have the following corollaries.

Corollary 1. *Consider perturbed CT-AZNN model (9) with the constant perturbation $\mathbf{p}(t) \in \mathbb{R}^{mn}$ of which the jth element $p_j(t) = c_j$ with c_j being constant with $j = 1, 2, \cdots, mn$. The perturbed CT-AZNN model (9) converges toward theoretical solution to CT-ASME (2).*

Corollary 2. *Consider perturbed CT-AZNN model (9) with the linear-form time-variant perturbation $\mathbf{p}(t) = \alpha t + \beta \in \mathbb{R}^{mn}$ of which the jth element $p_j(t) = \alpha_j t + \beta_j$ with α_j and β_j being constants with $j = 1, 2, \cdots, mn$. The perturbed CT-AZNN model (9) converges toward theoretical solution to CT-ASME (2) with residual error.*

Corollary 3. *Consider perturbed CT-AZNN model (9) with the sine-form time-variant perturbation $\mathbf{p}(t) = \alpha \sin(\beta(t-\omega)) \in \mathbb{R}^{mn}$ or the cosine-form time-variant perturbation $\mathbf{p}(t) = \alpha \cos(\beta(t-\omega)) \in \mathbb{R}^{mn}$ of which the jth element $p_j(t) = \alpha_j \sin(\beta_j(t-\omega_j))$ or $p_j(t) = \alpha_j \cos(\beta_j(t-\omega_j))$ with α_j, β_j and ω_j being constants with $j = 1, 2, \cdots, mn$. The perturbed CT-AZNN model (9) converges toward theoretical solution to CT-ASME (2) with residual error.*

Corollary 4. *Consider perturbed CT-AZNN model (9) with the exponential-decay-form time-variant perturbation* $\mathbf{p}(t) = \alpha \exp(-\beta t) + \omega \in \mathbb{R}^{mn}$ *of which the* j*th element* $p_j(t) = \alpha_j \exp(-\beta_j t) + \omega_j$ *with* α_j*,* β_j *and* ω_j *being constants and* $\beta_j > 0$ *with* $j = 1, 2, \cdots, mn$*. The perturbed CT-AZNN model (9) converges toward theoretical solution to CT-ASME (2) with residual error.*

In summary, the above theoretical results indicate the convergence performances of the proposed perturbed CT-AZNN model (9) for solving CT-ASME (2).

Remark 1. *Correspondingly, in the presence of perturbations, the CT-AZNN model (8) still possesses excellent performance. As shown in Theorem 1 and Corollary 1 through Corollary 4, the CT-AZNN model (8) can restrain all eligible perturbations with different steady-state residual errors. In fact, considering the Laplace transformation of the time-variant perturbation* $\mathbf{p}(t)$*, Theorem 1 implies the upper bound of perturbation suppression ability of CT-AZNN model (8). Generally speaking, if the time-variant growth rate of unknown perturbation is no more than linear-form time-variant perturbation* $\mathbf{p}(t) = \alpha t + \beta$*, the perturbed CT-AZNN model (9) can converge toward theoretical solution of CT-ASME (2) with residual error.*

3. Discretization formula and DT-AZNN model

In this section, a novel DT-AZNN model is proposed, developed and investigated for solving F-ASME (1).

3.1. 5-instant discretization formula

Recently published 5-instant discretization formula, which can be derived by exploiting Taylor expansion [41], is defined as follows [32, 42]:

$$\dot{u}_k = \frac{3}{7g}u_{k+1} + \frac{5}{42g}u_k - \frac{3}{7g}u_{k-1} - \frac{3}{14g}u_{k-2} + \frac{2}{21g}u_{k-3} + O(g^3), \qquad (11)$$

where the term $O(g^3)$ denotes the truncation error of the discretization formula. In addition, to show the performance of the sampling gap g involved in the discretization formula, we have the following property.

Property 1. *The optimal sampling gap* g *of above 5-instant discretization formula (11) is*

$$g = \left(\frac{18\varepsilon_{\max}}{49\kappa_{\max}}\right)^{\frac{1}{4}},$$

where $\varepsilon_{\max}$ *denotes the maximal absolute value of round-off errors and* $\kappa_{\max}$ *denotes the maximal absolute value of* $u^{(4)}(c_1)$, $u^{(4)}(c_2)$, $u^{(4)}(c_3)$ *and* $u^{(4)}(c_4)$.

Proof. Considering the existence of round-off errors in the numerical computations, the round-off errors in the 5-instant discretization formula (11) can be simplified as the following equations:

$$\begin{aligned} u_{k+1} &= v_{k+1} + \varepsilon_{k+1}; \\ u_k &= v_k + \varepsilon_k; \\ u_{k-1} &= v_{k-1} + \varepsilon_{k-1}; \\ u_{k-2} &= v_{k-2} + \varepsilon_{k-2}; \\ u_{k-3} &= v_{k-3} + \varepsilon_{k-3}, \end{aligned}$$

where u_{k+1}, u_k, u_{k-1}, u_{k-2} and u_{k-3} are approximated by numerical values v_{k+1}, v_k, v_{k-1}, v_{k-2} and v_{k-3}, respectively, and ε_{k+1}, ε_k, ε_{k-1}, ε_{k-2} and ε_{k-3} are the corresponding round-off errors. According to the 5-instant discretization formula (11), we obtain

$$\dot{u}_k = \frac{3}{7g}v_{k+1} + \frac{5}{42g}v_k - \frac{3}{7g}v_{k-1} - \frac{3}{14g}v_{k-2} + \frac{2}{21g}v_{k-3} + e_{\mathrm{r}} + e_{\mathrm{t}},$$

in which the term e_{r} denotes the round-off error and the term e_{t} denotes the truncation error. Furthermore, we have

$$e_{\mathrm{r}} = \left|\frac{3}{7g}\varepsilon_{k+1} + \frac{5}{42g}\varepsilon_k - \frac{3}{7g}\varepsilon_{k-1} - \frac{3}{14g}\varepsilon_{k-2} + \frac{2}{21g}\varepsilon_{k-3}\right| \leqslant \frac{9}{7g}\varepsilon_{\max}$$

and

$$e_{\mathrm{t}} = \left|\frac{1}{24}g^3u^{(4)}(c_1) - \frac{1}{24}g^3u^{(4)}(c_2) - \frac{1}{3}g^3u^{(4)}(c_3) + \frac{3}{4}g^3u^{(4)}(c_4)\right| \leqslant \frac{7}{6}g^3\kappa_{\max},$$

where c_1, c_2, c_3 and c_4 lie in $(kg, (k+1)g)$, $((k-1)g, kg)$, $((k-2)g, kg)$ and $((k-3)g, kg)$, respectively. In view of $\varepsilon_{\max}$ denoting the maximal absolute value of round-off errors of u_{k+1}, u_k, u_{k-1}, u_{k-2} and u_{k-3} as well as $\kappa_{\max}$ being a positive constant, it is known that $9\varepsilon_{\max}/(7g)$ is the upper bound of the round-off error e_{r}, and $7g^3\kappa_{\max}/6$ is the upper bound of the truncation error e_{t}. Thus, we have

$$|e_{\mathrm{r}} + e_{\mathrm{t}}| \leqslant \frac{9}{7g}\varepsilon_{\max} + \frac{7}{6}g^3\kappa_{\max}.$$

Note that floating-point numbers have limited precision in digital computer. For example, the precision of floating-point number in MATLAB environment is of order 10^{-16} (with its "eps" being 2.2×10^{-16}). Thus, the optimal sampling gap g of the 5-instant discretization formula (11) can be obtained as

$$g = \left(\frac{18\varepsilon_{\max}}{49\kappa_{\max}}\right)^{\frac{1}{4}}.$$

Based on the above analyses, the proof is thus completed. □

To substantiate the efficacy of the optimal sampling gap, we exploit the following function as the target function: $f(x) = \sin(x)$, and thus the first-order derivative of the target function is $f'(x) = \cos(x)$. Then, for the above target function, we have $\kappa_{\max} = 1$ and $\varepsilon_{\max} = 2.2 \times 10^{-16}$. Here, we use $x = 1$ as the target point in the following numerical experiment. At the target point, the errors between the theoretical value and the approximate value of the first-order derivative are presented in Table 1. As shown in Table 1, when the sampling gap g decreases, the value of the error decreases and then increases. Specifically, when the sampling gap $g = 7.5 \times 10^{-5}$ s, the minimal value of the error in approximation to the first-order derivative of the target function is coincident with the theoretical result.

Remark 2. *In this paper, as a further research of the 5-instant discretization formula (11), we derive the optimal sampling gap, which is an important property of the 5-instant discretization formula (11). As shown in Table 1, sampling gap* $g = 1 \times 10^{-4}$ s *can be seen as a demarcation line. Specifically, on the one hand, when the value of sampling gap* g *is greater than* 1×10^{-4} s*, the value of the error decreases by 1000 times when the sampling gap* g *decreases by 10 times, which is because when the value of* g *decreases, the truncation error* e_{t} *is dominant relative to round-off error* e_{r} *at this stage. On the other hand, when the value of sampling gap* g *is smaller than* 1×10^{-4} s*, the value of the error increases slightly, which is due to the nonnegligible influence of round-off error* e_{r} *relative to the truncation error* e_{t} *at this stage.*

3.2. Novel DT-AZNN model

Based on the above 5-instant discretization formula (11), a novel DT-AZNN model is investigated for F-ASME (1) solving. First of all, considering the proposed CT-AZNN model (8), we have the following theorem.

Table 1: Errors in approximation to $f(x) = \sin(x)$ using 5-instant discretization formula (11) with different values of sampling gap g (s).

Sampling gap g	Error	Sampling gap g	Error	Sampling gap g	Error
7.5×10^{-1}	3.0641×10^{-2}	7.5×10^{-4}	6.3336×10^{-11}	7.5×10^{-7}	5.0746×10^{-11}
5.0×10^{-1}	1.2788×10^{-2}	5.0×10^{-4}	1.8686×10^{-11}	5.0×10^{-7}	1.0895×10^{-10}
2.5×10^{-1}	2.0183×10^{-3}	2.5×10^{-4}	2.3150×10^{-12}	2.5×10^{-7}	2.5447×10^{-10}
1.0×10^{-1}	1.4269×10^{-4}	$\mathbf{1.0 \times 10^{-4}}$	$\mathbf{7.2387 \times 10^{-14}}$	1.0×10^{-7}	5.4551×10^{-10}
7.5×10^{-2}	6.1043×10^{-5}	7.5×10^{-5}	7.2342×10^{-13}	7.5×10^{-8}	7.9849×10^{-11}
5.0×10^{-2}	1.8329×10^{-5}	5.0×10^{-5}	1.0956×10^{-12}	5.0×10^{-8}	7.7834×10^{-10}
2.5×10^{-2}	2.3201×10^{-6}	2.5×10^{-5}	1.0956×10^{-12}	2.5×10^{-8}	5.4551×10^{-10}
1.0×10^{-2}	1.4965×10^{-7}	1.0×10^{-5}	1.6329×10^{-12}	1.0×10^{-8}	6.1334×10^{-9}
7.5×10^{-3}	6.3171×10^{-8}	7.5×10^{-6}	1.6329×10^{-12}	7.5×10^{-9}	2.4082×10^{-9}
5.0×10^{-3}	1.8739×10^{-8}	5.0×10^{-6}	8.9089×10^{-12}	5.0×10^{-9}	1.4356×10^{-8}
2.5×10^{-3}	2.3451×10^{-9}	2.5×10^{-6}	3.8241×10^{-12}	2.5×10^{-9}	3.1798×10^{-9}
1.0×10^{-3}	1.5011×10^{-10}	1.0×10^{-6}	5.0746×10^{-11}	1.0×10^{-9}	8.8861×10^{-8}

Theorem 2. *The DT-AZNN model is formulated as follows:*

$$\begin{aligned}\mathbf{x}_{k+1} =& -\frac{7}{3}M_k^{-1}\left(2h\left(M_k\mathbf{x}_k - \mathbf{e}_k\right) + (h^2/g)\mathbf{y}_k + g\dot{M}_k\mathbf{x}_k - g\dot{\mathbf{e}}_k\right) \\ & - \frac{5}{18}\mathbf{x}_k + \mathbf{x}_{k-1} + \frac{1}{2}\mathbf{x}_{k-2} - \frac{2}{9}\mathbf{x}_{k-3} + \mathbf{O}(g^4),\end{aligned} \tag{12}$$

where $M_k = B_k^{\mathrm{T}} \otimes A_k + D_k^{\mathrm{T}} \otimes C_k$*;* $\dot{M}_k = B_k^{\mathrm{T}} \otimes \dot{A}_k + \dot{B}_k^{\mathrm{T}} \otimes A_k + D_k^{\mathrm{T}} \otimes \dot{C}_k + \dot{D}_k^{\mathrm{T}} \otimes C_k$*; variables* $\mathbf{x}_k$ *and* $\mathbf{e}_k$ *denote the vectorization of* X_k *and* E_k*, respectively;* $h = \mu g$ *denotes the step length; term* $\mathbf{O}(g^4)$ *denotes the truncation error matrix with each element being* $O(g^4)$*.*

Proof. According to the definitions of $\dot{\mathbf{z}}(t)$, $\mathbf{z}(t)$ and $\int_0^t \mathbf{z}(\sigma)\mathrm{d}\sigma$, the AZNN design formula (5) can be discretized as

$$\dot{\mathbf{z}}_k = -2\mu\mathbf{z}_k - \mu^2\mathbf{y}_k,$$

which can be rewritten as

$$\dot{M}_k\mathbf{x}_k + M_k\dot{\mathbf{x}}_k - \dot{\mathbf{e}}_k = -2\mu(M_k\mathbf{x}_k - \mathbf{e}_k) - \mu^2\mathbf{y}_k,$$

where

$$\mathbf{y}_k = \frac{7}{3}g\mathbf{z}_{k-1} - \frac{5}{18}\mathbf{y}_{k-1} + \mathbf{y}_{k-2} + \frac{1}{2}\mathbf{y}_{k-3} - \frac{2}{9}\mathbf{y}_{k-4} + \mathbf{O}(g^4).$$

Considering that the discrete-form of time-variant matrix M_k is nonsingular for all duration time $[0, t_{\mathrm{f}}] \subseteq [0, +\infty)$, the following equation is obtained:

$$\dot{\mathbf{x}}_k = M_k^{-1}\left(-2\mu(M_k\mathbf{x}_k - \mathbf{e}_k) - \mu^2\mathbf{y}_k - \dot{M}_k\mathbf{x}_k + \dot{\mathbf{e}}_k\right).$$

Applying the 5-instant discretization formula (11) to above equation yields, we have

$$\begin{aligned}&\frac{3}{7g}\mathbf{x}_{k+1} + \frac{5}{42g}\mathbf{x}_k - \frac{3}{7g}\mathbf{x}_{k-1} - \frac{3}{14g}\mathbf{x}_{k-2} + \frac{2}{21g}\mathbf{x}_{k-3} + \mathbf{O}(g^3)\\ =&M_k^{-1}\left(-2\mu(M_k\mathbf{x}_k - \mathbf{e}_k) - \mu^2\mathbf{y}_k - \dot{M}_k\mathbf{x}_k + \dot{\mathbf{e}}_k\right).\end{aligned}$$

Thus, we further have the following DT-AZNN model:

$$\begin{aligned}\mathbf{x}_{k+1} =& -\frac{7}{3}M_k^{-1}\left(2h\left(M_k\mathbf{x}_k - \mathbf{e}_k\right) + (h^2/g)\mathbf{y}_k + g\dot{M}_k\mathbf{x}_k - g\dot{\mathbf{e}}_k\right)\\ &- \frac{5}{18}\mathbf{x}_k + \mathbf{x}_{k-1} + \frac{1}{2}\mathbf{x}_{k-2} - \frac{2}{9}\mathbf{x}_{k-3} + \mathbf{O}(g^4).\end{aligned}$$

The proof is thus completed. □

For the convenience of further discussions and theoretical analyses, based on the recent research [32], the following properties about DT-AZNN model (12) are provided, which theoretically demonstrate its 0-stability, consistency and convergence performance for solving F-ASME (1) in the absence of perturbations.

Property 2. *The DT-AZNN model (12) is 0-stable, consistent and convergent with the truncating error of the order* $\mathbf{O}(g^4)$.

Proof. According to the Result 1 in [32], the solutions of characteristic polynomial include two real roots and a couple of conjugate imaginary roots (i.e., $\varsigma_1 = 1$, $\varsigma_2 = 0.2976$, $\varsigma_3 = -0.7877 + 0.3552\mathrm{i}$ and $\varsigma_4 = -0.7877 - 0.3552\mathrm{i}$, where i denotes imaginary unit). Evidently, these roots are in the unit circle, and only one root (i.e., $\varsigma_1 = 1$) is on the unit circle, then the proposed DT-AZNN model (12) is 0-stable. Furthermore, based on the Theorem 2, the truncation error of DT-AZNN model (12) is $\mathbf{O}(g^4)$. Therefore, according to Result 2 in [32], the proposed DT-AZNN model (12) is said to be consistent of order 4. According to Results 3 and 4 in [32], the proposed DT-AZNN model (12) is 0-stable and consistent, which converges with the truncating error of the order $\mathbf{O}(g^4)$. The proof is thus completed. □

Property 3. *The maximal steady-state residual error* $\|M_{k+1}\mathbf{x}_{k+1}-\mathbf{e}_{k+1}\|_2$ *of the proposed DT-AZNN model (12) is of the order* $O(g^4)$ *with symbol* $\|\cdot\|_2$ *denoting the Euclidean norm of a vector.*

Proof. Let $\mathbf{x}^*_{k+1}$ denote the vectorization of X^*_{k+1}, which is the theoretical solution of F-ASME (1). In this sense, it can be obtained that $M_{k+1}\mathbf{x}^*_{k+1}-\mathbf{e}_{k+1}=\mathbf{0}$. Moreover, according to the Theorem 2, $\mathbf{x}_{k+1}=\mathbf{x}^*_{k+1}+\mathbf{O}(g^4)$ for $k\to+\infty$. Therefore, we have

$$\begin{aligned}
&\lim_{k\to+\infty}\sup\|M_{k+1}\mathbf{x}_{k+1}-\mathbf{e}_{k+1}\|_2\\
=&\lim_{k\to+\infty}\sup\left\|M_{k+1}\mathbf{x}^*_{k+1}-\mathbf{e}_{k+1}+M_{k+1}\mathbf{O}(g^4)\right\|_2\\
=&\lim_{k\to+\infty}\sup\left\|M_{k+1}\mathbf{O}(g^4)\right\|_2\\
\leq&\lim_{k\to+\infty}\sup\|M_{k+1}\|_{\mathrm{F}}O(g^4)\\
=&O(g^4),
\end{aligned}$$

where $\|\cdot\|_{\mathrm{F}}$ denotes the Frobenius norm of a matrix. Thus, the maximal steady-state residual error of the proposed DT-AZNN model (12) is of the order $O(g^4)$. The proof is thus completed. □

The above Property 2 and Property 3 show that the proposed DT-AZNN model (12) converges toward the theoretical solution of F-ASME (1). Furthermore, considering the effect of kinds of perturbations, the perturbed DT-AZNN model can be obtained as

$$\begin{aligned}
\mathbf{x}_{k+1}=&-\frac{7}{3}M_k^{-1}\Big(2h\left(M_k\mathbf{x}_k-\mathbf{e}_k\right)+(h^2/g)\mathbf{y}_k+g\dot{M}_k\mathbf{x}_k-g\dot{\mathbf{e}}_k-g\mathbf{p}_k\Big)\\
&-\frac{5}{18}\mathbf{x}_k+\mathbf{x}_{k-1}+\frac{1}{2}\mathbf{x}_{k-2}-\frac{2}{9}\mathbf{x}_{k-3}+\mathbf{O}(g^4),
\end{aligned}\tag{13}$$

where $\mathbf{p}_k$ denotes the discrete-form of the time-variant perturbation vector. Moreover, the following theoretical analyses further reveal the superior performance of the proposed DT-AZNN model (12).

Corollary 5. *Consider perturbed DT-AZNN model (13) with the constant perturbation* $\mathbf{p}_k=\mathbf{c}\in\mathbb{R}^{mn}$ *of which the* j*th element* $p^k_j=c_j$ *with* c_j *being constant with* $j=1,2,\cdots,mn$. *The perturbed DT-AZNN model (13) converges toward theoretical solution of F-ASME (1) with residual error.*

Corollary 6. *Consider perturbed DT-AZNN model (13) with the linear-form time-variant perturbation* $\mathbf{p}_k = \alpha t_k + \beta \in \mathbb{R}^{mn}$ *of which the* j*th element* $p_j^k = \alpha_j t_k + \beta_j$ *with* α_j *and* β_j *being constants with* $j = 1, 2, \cdots, mn$*. The perturbed DT-AZNN model (13) converges toward theoretical solution of F-ASME (1) with residual error.*

Corollary 7. *Consider perturbed DT-AZNN model (13) with the sine-form time-variant perturbation* $\mathbf{p}_k = \alpha \sin(\beta(t_k - \omega)) \in \mathbb{R}^{mn}$ *or cosine-form time-variant perturbation* $\mathbf{p}_k = \alpha \cos(\beta(t_k - \omega)) \in \mathbb{R}^{mn}$ *of which the* j*th element* $p_j^k = \alpha_j \sin(\beta_j(t_k - \omega_j))$ *or* $p_j^k = \alpha_j \cos(\beta_j(t_k - \omega_j))$ *with* α_j*,* β_j *and* ω_j *being constants with* $j = 1, 2, \cdots, mn$*. The perturbed DT-AZNN model (13) converges toward theoretical solution of F-ASME (1) with residual error.*

Corollary 8. *Consider perturbed DT-AZNN model (13) with the exponential-decay-form time-variant perturbation* $\mathbf{p}_k = \alpha \exp(-\beta t_k) + \omega \in \mathbb{R}^{mn}$ *of which the* j*th element* $p_j^k = \alpha_j \exp(-\beta_j t_k) + \omega_j$ *with* α_j*,* β_j *and* ω_j *being constants and* $\beta_j > 0$ *with* $j = 1, 2, \cdots, mn$*.. The perturbed DT-AZNN model (13) converges toward theoretical solution of F-ASME (1) with residual error.*

Remark 3. *Considering DT-AZNN model (12), in the absence of perturbations, the computational precision is mainly affected by the discretization formula; in the presence of perturbations, the computational precision is mainly affected by the ability of perturbation suppression of the model [32]. Generally speaking, for the model with poor stability, slight perturbations may generate relatively serious distortion of steady-state residual error, which means the generated solutions synthesized by the model can not converge to the theoretical ones with a satisfying computational precision. As the analyses presented in Theorem 1, the proposed CT-AZNN model (8) can suppress the continuous-form of time-variant perturbations effectively, and then the corresponding DT-AZNN model (12) can also suppress the discrete-form of time-variant perturbations with appropriate sampling gap* g*. Specifically, as shown in Corollary 6, given the perturbed DT-AZNN model (13) with linear-form time-variant perturbation* $\mathbf{p}_k = \alpha t_k + \beta \in \mathbb{R}^{mn}$*, we have* $\lim_{k\to\infty} \sup \|\mathbf{e}(t_{k+1})\|_2 = \|\alpha\|_2/\mu^2 + O(g^4) = \|\alpha\|_2 g^2/h^2 + O(g^4) = O(g^2)$ *[32], which shows that the computational precision is mainly affected by the ability of perturbation suppression of model rather than the discretization formula.*

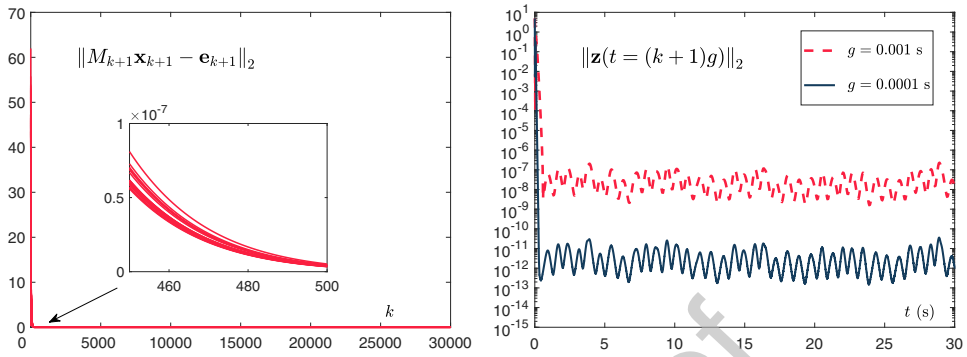

(a) (b)

Figure 1: Residual errors synthesized by proposed DT-AZNN model (12) for solving F-ASME (14) in absence of perturbations. (a) Residual errors synthesized by DT-AZNN model (12) with $g = 0.001$ s and randomly-generated initial states. (b) Residual errors synthesized by DT-AZNN model (12) with different values of g.

4. Numerical experiments and comparisons

In this section, the comparative numerical experiments are presented for substantiating the effectiveness and robustness of the proposed DT-AZNN model (12). First of all, without loss of generality, consider the following F-ASME with X_{k+1} to be computed at each computational time interval $[kg, (k+1)g) \subseteq [0, 30]$:

$$A_{k+1}X_{k+1}B_{k+1} + C_{k+1}X_{k+1}D_{k+1} = E_{k+1}, \tag{14}$$

where

$$A_k = \begin{bmatrix} a_{11}(t_k) & a_{12}(t_k) & \cdots & a_{1m}(t_k) \\ a_{21}(t_k) & a_{22}(t_k) & \cdots & a_{2m}(t_k) \\ \vdots & \vdots & \ddots & \vdots \\ a_{m1}(t_k) & a_{m1}(t_k) & \cdots & a_{mm}(t_k) \end{bmatrix} \in \mathbb{R}^{m\times m};$$

$$B_k = \begin{bmatrix} b_{11}(t_k) & b_{12}(t_k) & \cdots & b_{1n}(t_k) \\ b_{21}(t_k) & b_{22}(t_k) & \cdots & b_{2n}(t_k) \\ \vdots & \vdots & \ddots & \vdots \\ b_{n1}(t_k) & b_{n1}(t_k) & \cdots & b_{nn}(t_k) \end{bmatrix} \in \mathbb{R}^{n\times n};$$

$$C_k = \begin{bmatrix} c_{11}(t_k) & c_{12}(t_k) & \cdots & c_{1m}(t_k) \\ c_{21}(t_k) & c_{22}(t_k) & \cdots & c_{2m}(t_k) \\ \vdots & \vdots & \ddots & \vdots \\ c_{m1}(t_k) & c_{m1}(t_k) & \cdots & c_{mm}(t_k) \end{bmatrix} \in \mathbb{R}^{m\times m};$$

$$D_k = \begin{bmatrix} d_{11}(t_k) & d_{12}(t_k) & \cdots & d_{1n}(t_k) \\ d_{11}(t_k) & d_{12}(t_k) & \cdots & d_{1n}(t_k) \\ \vdots & \vdots & \ddots & \vdots \\ d_{n1}(t_k) & d_{n1}(t_k) & \cdots & d_{nn}(t_k) \end{bmatrix} \in \mathbb{R}^{n\times n};$$

$$E_k = \begin{bmatrix} e_{11}(t_k) & e_{12}(t_k) & \cdots & e_{1n}(t_k) \\ e_{11}(t_k) & e_{12}(t_k) & \cdots & e_{1n}(t_k) \\ \vdots & \vdots & \ddots & \vdots \\ e_{m1}(t_k) & e_{m1}(t_k) & \cdots & e_{mn}(t_k) \end{bmatrix} \in \mathbb{R}^{m\times n}.$$

Thereinto,

$$a_{ij} = \begin{cases} 5 + \cos((5/2)t_k), & \text{for } i = j \\ (2/3)\sin((3/2)t_k)/(i-j), & \text{for } i > j \\ (2/3)\sin((3/2)t_k)/(j-i), & \text{for } i < j, \end{cases}$$

$$b_{ij} = \begin{cases} \sin(2t_k), & \text{for } i = j \\ -\cos(2t_k), & \text{for } i > j \\ \cos(2t_k), & \text{for } i < j, \end{cases}$$

$$c_{ij} = \begin{cases} 2 + \sin(t_k), & \text{for } i = j \\ \cos(t_k)/(i-j), & \text{for } i > j \\ \cos(t_k)/(j-i), & \text{for } i < j, \end{cases}$$

$$d_{ij} = \begin{cases} (1/2)\sin(t_k), & \text{for } i = j \\ -(1/2)\cos(t_k), & \text{for } i > j \\ (1/2)\cos(t_k), & \text{for } i < j, \end{cases}$$

and

$$e_{ij} = \begin{cases} \sin(0.15t), & \text{for } \mathrm{rem}(i) = 1,\ j \text{ being odd} \\ \cos(0.15t), & \text{for } \mathrm{rem}(i) = 1,\ j \text{ being even} \\ \cos(0.2t) + 1, & \text{for } \mathrm{rem}(i) = 2,\ j \text{ being odd} \\ \sin(0.2t) + 1, & \text{for } \mathrm{rem}(i) = 2,\ j \text{ being even} \\ \cos(0.2t)\sin(0.25t), & \text{for } \mathrm{rem}(i) = 3, \end{cases}$$

with $\mathrm{rem}(\cdot)$ denoting the remainder operation.

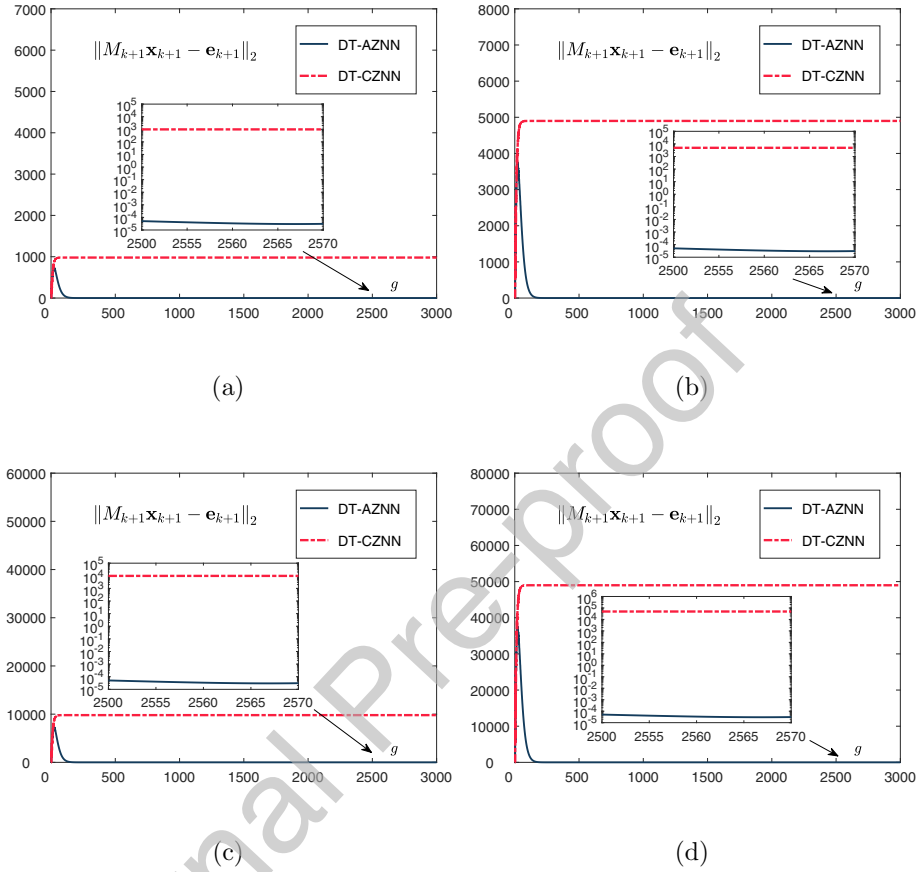

Figure 2: Residual errors synthesized by perturbed DT-AZNN model (13) and perturbed DT-CZNN model (15) for solving F-ASME (14) with $\gamma = 5$ and $g = 0.01$ s in presence of constant perturbations. (a) Constant perturbation $gp_j^k = 20$. (b) Constant perturbation $gp_j^k = 100$. (c) Constant perturbation $gp_j^k = 200$. (d) Constant perturbation $gp_j^k = 1000$.

For convenience, in this paper, we set the parameters of matrix dimensions $m = 6$ and $n = 4$. First of all, the fundamental numerical experimental results synthesized by DT-AZNN model (12) for solving F-ASME (14) are shown in Figure 1. On the one hand, without loss of generality, starting from 20 randomly-generated initial states of $\mathbf{x}_0 \in [0, 1]^{24\times 1}$ and $\mathbf{y}_0 = \mathbf{0} \in \mathbb{R}^{24\times 1}$, we use the conventional Euler method to compute the other initial states. As seen from Figure 1(a), the state trajectories of residual errors

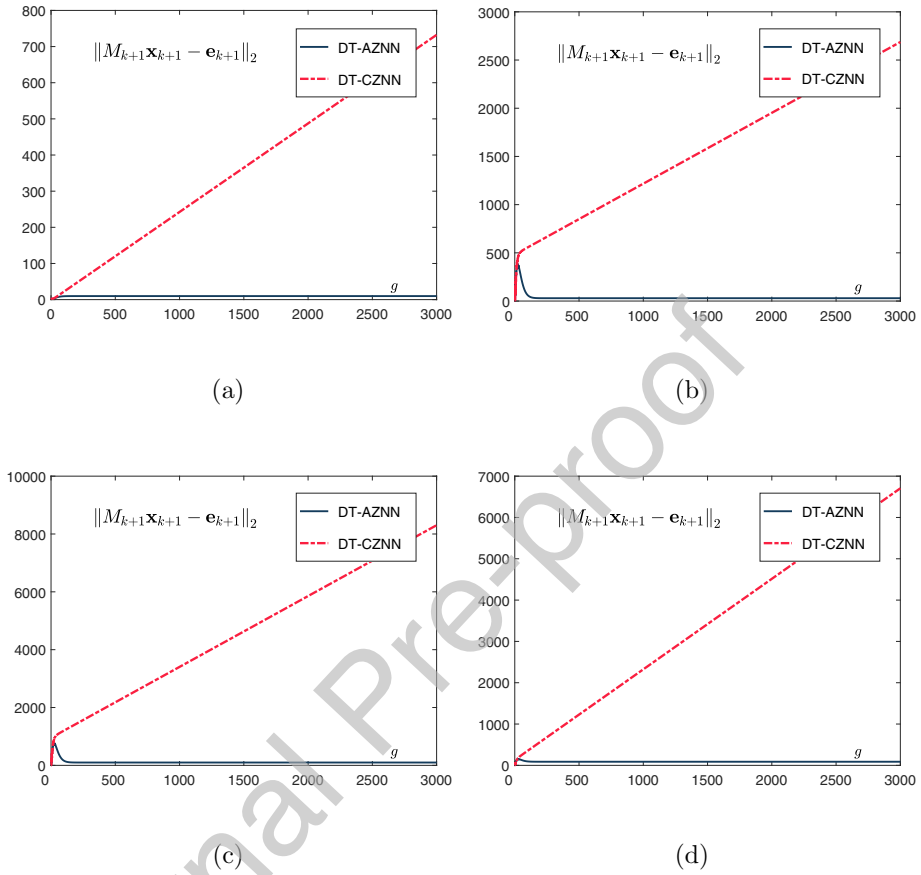

Figure 3: Residual errors synthesized by perturbed DT-AZNN model (13) and perturbed DT-CZNN model (15) for solving F-ASME (14) with $\gamma = 5$ and $g = 0.01$ s in presence of linear-form time-variant perturbations. (a) Linear-form time-variant perturbation $gp_j^k = 0.5t_k$. (b) Linear-form time-variant perturbation $gp_j^k = 1.5t_k + 10$. (c) Linear-form time-variant perturbation $gp_j^k = 5t_k + 20$. (d) Linear-form time-variant perturbation $gp_j^k = 2\sqrt{5}t_k + \sqrt{10}$.

$\|M_{k+1}\mathbf{x}_{k+1} - \mathbf{e}_{k+1}\|_2$ always converge to near zero accurately and rapidly, which means that the obtained solutions always converge to the theoretical solution. On the other hand, for comparison convenience, starting from initial states of $\mathbf{x}_0 = \mathbf{0} \in \mathbb{R}^{24\times 1}$ and $\mathbf{y}_0 = \mathbf{0} \in \mathbb{R}^{24\times 1}$, we also use the conventional Euler method to compute the other initial states, and set the parameter of integral part of the DT-AZNN model (12) as 1 (i.e., $h^2/g = 1$). As

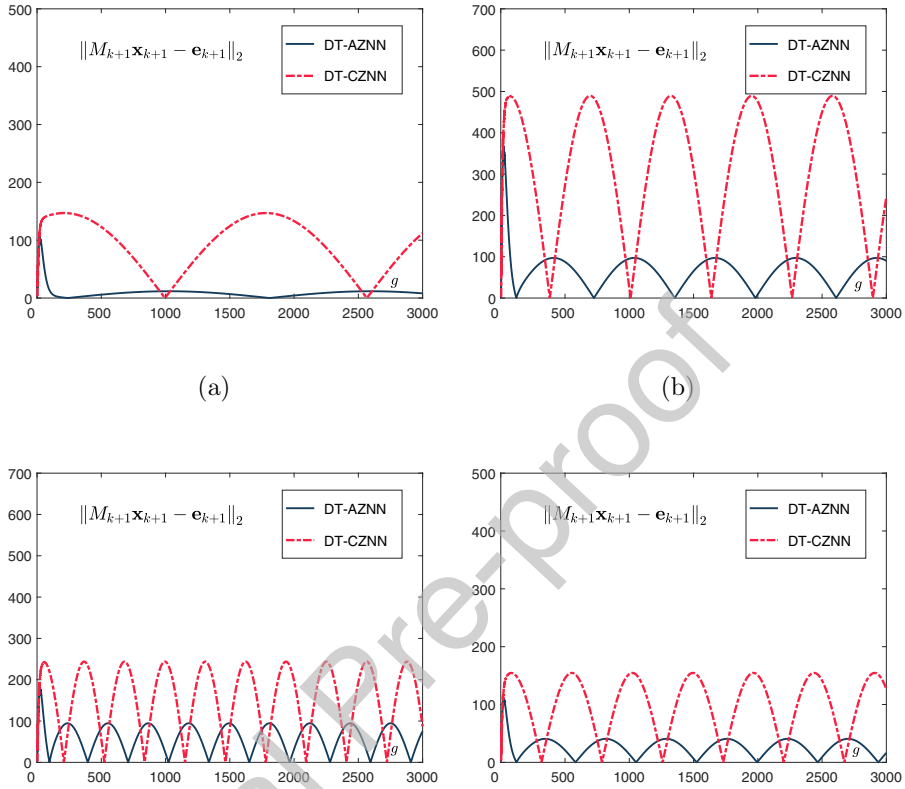

Figure 4: Residual errors synthesized by perturbed DT-AZNN model (13) and perturbed DT-CZNN model (15) for solving F-ASME (14) with $\gamma = 5$ and $g = 0.01$ s in presence of sine-form time-variant perturbation and cosine-form time-variant perturbations. (a) Sine-form time-variant perturbation $gp_j^k = 10\sin(0.5(t_k - 10))$. (b) Cosine-form time-variant perturbation $gp_j^k = 3\cos(0.2(t_k - 2))$. (c) Sine-form time-variant perturbation $gp_j^k = 5\sin(t_k+20)$. (d) Cosine-form time-variant perturbation $gp_j^k = \sqrt{10}\cos(2/3(t_k+4))$.

illustrated in Figure 1(b), we can see that the maximal steady-state residual error of the proposed DT-AZNN model (12) changes in the manner of $O(g^4)$ approximatively, which coincides with the aforementioned theoretical results.

Secondly, to further illustrate the perturbations suppression performance of the proposed DT-AZNN model (12), the perturbed discrete-time classical

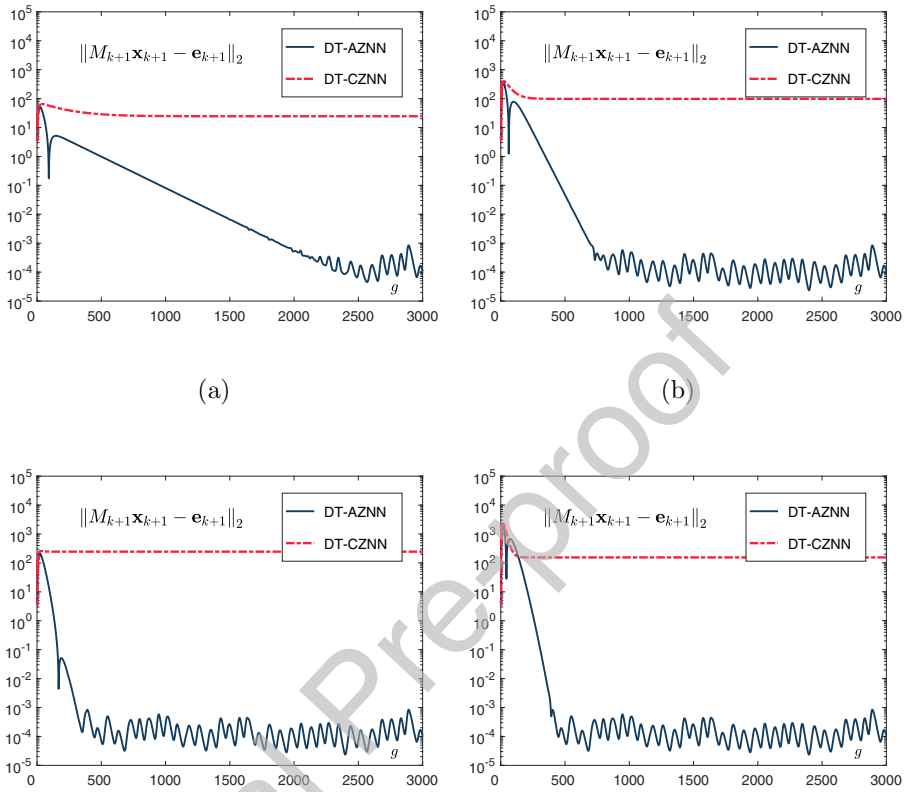

Figure 5: Residual errors synthesized by perturbed DT-AZNN model (13) and perturbed DT-CZNN model (15) for solving F-ASME (14) with $\gamma = 5$ and $g = 0.01$ s in presence of exponential-decay-form time-variant perturbations. (a) Exponential-decay-form time-variant perturbation $gp_j^k = \exp(-0.5t_k) + 0.5$. (b) Exponential-decay-form time-variant perturbation $gp_j^k = 10\exp(-2t_k) + 2$. (c) Exponential-decay-form time-variant perturbation $gp_j^k = 2\exp(-6t_k) + 5$. (d) Exponential-decay-form time-variant perturbation $gp_j^k = 100\exp(-5t_k) + \sqrt{10}$.

zeroing neural network (DT-CZNN) model introduced in [32, 42] is presented

here for comparison, which is designed as

$$\begin{aligned}\mathbf{x}_{k+1} = &-\frac{7}{3}M_k^{-1}\left(2h\left(M_k\mathbf{x}_k-\mathbf{e}_k\right)+g\dot{M}_k\mathbf{x}_k-g\dot{\mathbf{e}}_k-g\mathbf{p}_k\right)\\ &-\frac{5}{18}\mathbf{x}_k+\mathbf{x}_{k-1}+\frac{1}{2}\mathbf{x}_{k-2}-\frac{2}{9}\mathbf{x}_{k-3}+\mathbf{O}(g^4).\end{aligned} \tag{15}$$

Here, starting from initial states of $\mathbf{x}_0 = \mathbf{0} \in \mathbb{R}^{24\times 1}$ and $\mathbf{y}_0 = \mathbf{0} \in \mathbb{R}^{24\times 1}$, we also use the conventional Euler method to compute the other initial states, and fix the parameter γ and sampling gap g (i.e., $\gamma = 5$ and $g = 0.01$ s). The residual errors of the perturbed DT-AZNN model (13) (denoted by mazarine solid curve) and the perturbed DT-CZNN model (15) (denoted by red dash-dotted curve) are illustrated in Figure 2 through Figure 5. These numerical experiments indicate that the proposed DT-AZNN model (12) is effective (in terms of a relatively tiny residual error) on F-ASME (14) solving with time-variant perturbations suppressed. Specifically, the following analyses are obtained as shown in Figure 2 through Figure 5.

1) As shown in Figure 2, consider the constant perturbations $gp_j^k = 20$, $gp_j^k = 100$, $gp_j^k = 200$ and $gp_j^k = 1000$ with $j = 1, 2, \cdots, 24$, the perturbed DT-AZNN model (13) converges toward the theoretical solution of F-ASME (14) with a tiny residual error. Whereas, the residual errors synthesized by the perturbed DT-CZNN model (15) remain at relative large level, which are approximately 10^7 times through 10^9 times (with different constant perturbations) larger than those synthesized by the perturbed DT-AZNN model (13). These results illustrate that the perturbed DT-CZNN model (15) can not converge to the theoretical solution of F-ASME (14) in the presence of constant perturbations.

2) As shown in Figure 3, consider the linear-form time-variant perturbations $gp_j^k = 0.5t_k$, $gp_j^k = 1.5t_k + 10$, $gp_j^k = 5t_k + 20$ and $gp_j^k = 2\sqrt{5}t_k + \sqrt{10}$ with $j = 1, 2, \cdots, 24$, the perturbed DT-AZNN model (13) converges toward the theoretical solution of F-ASME (14) with a stabilize residual error, while the residual error of the perturbed DT-CZNN model (15) keeps increasing with the time. This means that the proposed DT-AZNN model (12) can suppress the linear-form time-variant perturbation efficiently.

3) As shown in Figure 4, consider the sine-form time-variant perturbations $gp_j^k = 10\sin(0.5(t_k - 10))$ and $gp_j^k = 5\sin(t_k + 20)$ as well as

the cosine-form time-variant perturbations $gp_j^k = 3\cos(0.2(t_k - 2))$ and $gp_j^k = \sqrt{10}\cos(2/3(t_k + 4))$ with $j = 1, 2, \cdots, 24$, the perturbed DT-AZNN model (13) and the perturbed DT-CZNN model (15) all converge toward the theoretical solution of F-ASME (14) with periodic fluctuations. However, it is evident that the maximum steady-state residual errors of perturbed DT-CZNN model (15) are larger than those of the perturbed DT-AZNN model (13), which means that the computational performance of the latter model is better than the former model.

4) As shown in Figure 5, consider the exponential-decay-form time-variant perturbations $gp_j^k = \exp(-0.5t_k) + 0.5$, $gp_j^k = 10\exp(-2t_k) + 2$, $gp_j^k = 2\exp(-6t_k) + 5$ and $gp_j^k = 100\exp(-5t_k) + \sqrt{10}$ with $j = 1, 2, \cdots, 24$, the perturbed DT-AZNN model (13) converges toward the theoretical solution of F-ASME (14) with a tiny residual error, and the perturbed DT-CZNN model (15) can not converge toward the theoretical solution of F-ASME (14). In fact, the determinate exponential-decay-form time-variant perturbations tend to a constant value with time, and thus the discussions on the performance of the models (13) and (15) can refer to 1).

In summary, above comparative numerical experimental results in accord with the theoretical analyses offered in Section 3 further substantiate the effectiveness and robustness of the proposed DT-AZNN model (12) for solving F-ASME (14) in comparison with the classical model.

5. Conclusion

In this paper, a novel DT-AZNN model (12) has been proposed, developed and investigated for solving F-ASME (1). Specifically, first of all, based on the Kronecker product and the vectorization operation, the CT-ASME (2) has been transformed into a simple continuous-time linear system. By exploiting the AZNN design formula (5), a CT-AZNN model (8) has been developed and presented for solving time-variant linear system. Secondly, the theoretical analysis about the optimal sampling gap of the 5-instant discretization formula has been provided. Then, by exploiting the 5-instant discretization formula to discretize the CT-AZNN model (8), a novel DT-AZNN model (12) has been designed and generalized for solving F-ASME (1). Note

that the proposed models (8) and (12) keep efficient and robustness in the presence of perturbations. Furthermore, the comparative numerical experiments have been conducted to substantiate the superior convergence performance and robustness of the proposed DT-AZNN model (12). In the future researches, we will mainly focus on investigating a series of derived problems, e.g., future unknown-transpose matrix. Moreover, more comparisons between the recently published ZNN models and the other related methods are also significant.

References

[1] E. B. Castelan and V. G. Silva, On the solution of a Sylvester equation appearing in descriptor systems control theory, Syst. Control Lett. 54 (2005) 109–117.

[2] Q. Qi, H. Zhang, and Z. Wu, Stabilization control for linear continuous-time mean-field systems, IEEE Trans. Autom. Control 64 (8) (2019) 3461–3468.

[3] Q. Qi, H. Zhang, and Z. Ji, Further results on stabilization for NCSs with packet losses and transmission delay: UDP case, J. Franklin Inst. 356 (8) (2019) 4601–4621.

[4] Q. Wang, Z. He, and Y. Zhang, Constrained two-sided coupled Sylvester-type quaternion matrix equations, Automatica 101 (2019) 207–213.

[5] L. Jin and S. Li, Distributed task allocation of multiple robots: A control perspective, IEEE Trans. Syst. Man. Cybern. Syst. 48 (5) (2018) 693–701.

[6] B. Liao, Q. Xiang, and S. Li, Bounded Z-type neurodynamics with limited-time convergence and noise tolerance for calculating time-dependent Lyapunov equation, Neurocomputing 325 (24) (2019) 234–241.

[7] R. H. Bartels and G. W. Stewart, Solution of the matrix equation $AX + XB = C$, Commun. ACM 15 (9) (1972) 820–826.

[8] M. Monsalve, Block linear method for large scale Sylvester equations, Comput. Appl. Math. 27 (1) (2008) 47–59.

[9] S. Li and Y. Li, Nonlinearly activated neural network for solving time-varying complex Sylvester equation, IEEE Trans. Cybern. 44 (8) (2014) 1397–1407.

[10] X. Yan, M. Liu, L. Jin, S. Li, B. Hu, X. Zhang, and Z. Huang, New zeroing neural network models for solving nonstationary Sylvester equation with verifications on mobile manipulators, IEEE Trans. Ind. Inf. 15 (9) (2019) 5011–5022.

[11] Y. Zhang, D. Jiang, and J. Wang, A recurrent neural network for solving Sylvester equation with time-varying coefficients, IEEE Trans. Neural Networks 13 (5) (2002) 1053–1063.

[12] K. Chen, Improved neural dynamics for online Sylvester equations solving, Inf. Process. Lett. 116 (7) (2016) 455–459.

[13] S. Li, S. Chen, and B. Liu, Accelerating a recurrent neural network to finite-time convergence for solving time-varying Sylvester equation by using a sign-bi-power activation function, Neural Process. Lett. 37 (2) (2013) 189–205.

[14] L. Xiao, B. Liao, S. Li, and K. Chen, Nonlinear recurrent neural networks for finite-time solution of general time-varying linear matrix equations, Neural Netw. 98 (2018) 102–113.

[15] L. Xiao, Z. Zhang, Z. Zhang, W. Li, and S. Li, Design, verification and robotic application of a novel recurrent neural network for computing dynamic Sylvester equation, Neural Netw. 105 (2018) 185–196.

[16] Z. Zhang, L. Zheng, J. Weng, Y. Mao, W. Lu, and L. Xiao, A new varying-parameter recurrent neural-network for online solution of time-varying Sylvester equation, IEEE Trans. Cybern. 48 (11) (2018) 3135–3148.

[17] Z. Yin, K. Liu, Y. Chen, R. Xue, J. Li, and Y. Shi, Performance analyses of four-instant discretization formulas with application to generalized-Sylvester-type future matrix equation, IEEE Access 7 (2019) 152258–152266.

[18] F. Xu, Z. Li, Z. Nie, H. Shao, and D. Guo, Zeroing neural network for solving time-varying linear equation and inequality systems, IEEE Trans. Neural Networks Learn. Sys. 30 (8) (2019) 2346–2357.

[19] L. Xiao and R. Lu, Finite-time solution to nonlinear equation using recurrent neural dynamics with a specially-constructed activation function, Neurocomputing 151 (1) (2015) 246–251.

[20] L. Jin, S. Li, and B. Hu, RNN models for dynamic matrix inversion: a control-theoretical perspective, IEEE Trans. Ind. Inf. 14 (1) (2018) 189–199.

[21] S. Li, B. Liu, and Y. Li, Selective positive-negative feedback produces the winner-take-all competition in recurrent neural networks, IEEE Trans. Neural Networks Learn. Sys. 24 (2) (2013) 301–309.

[22] J. Zhang, L. Jin, and L. Cheng RNN for perturbed manipulability optimization of manipulators based on a distributed scheme: A game-theoretic perspective, IEEE Trans. Neural Networks Learn. Sys. In Press DOI 10.1109/TNNLS.2020.2963998

[23] L. Jin, J. Yan, X. Du, X. Xiao, and D. Fu, RNN for solving time-variant generalized Sylvester equation with applications to robots and acoustic source localization, IEEE Trans. Ind. Inf. In Press DOI: 10.1109/TII.2020.2964817

[24] J. Na, Q. Chen, X. Ren, and Y. Guo, Adaptive prescribed performance motion control of servo mechanisms with friction compensation, IEEE Trans. Ind. Electron. 61 (1) (2014) 486–494.

[25] L. Jin, S. Li, B. Liao, and Z. Zhang, Zeroing neural networks: A survey, Neurocomputing 267 (6) (2017) 597–604.

[26] D. Guo and Y. Zhang, Novel recurrent neural network for time-varying problems solving, IEEE Comput. Intell. Mag. 7 (4) (2012) 61–65.

[27] L. Xiao, Accelerating a recurrent neural network to finite-time convergence using a new design formula and its application to time-varying matrix square root, J. Franklin Inst. 354 (13) (2017) 5667–5677.

[28] Y. Shi, B. Qiu, D. Chen, J. Li, and Y. Zhang, Proposing and validation of a new 4-point finite difference formula with manipulator application, IEEE Trans. Ind. Inf. 14 (4) (2018) 1323–1333.

[29] L. Jin, Y. Zhang, S. Li, and Y. Zhang, Modified ZNN for time-varying quadratic programming with inherent tolerance to noises and its application to kinematic redundancy resolution of robot manipulators, IEEE Trans. Ind. Electron. 63 (11) (2016) 6978–6988.

[30] L. Jin, Y. Zhang, and S. Li, Integration-enhanced Zhang neural network for real-time-varying matrix inversion in the presence of various kinds of noises, IEEE Trans. Neural Networks Learn. Sys. 27 (12) (2016) 2615–2627.

[31] Y. Shi and Y. Zhang, Discrete time-variant nonlinear optimization and system solving via integral-type error function and twice ZND formula with noises suppressed, Soft Comput. 22 (21) (2018) 7129–7141.

[32] Y. Shi and Y. Zhang, Solving future equation systems using integral-type error function and using twice ZNN formula with disturbances suppressed, J. Franklin Inst. 356 (4) (2019) 2130–2152.

[33] M. Hajarian, Convergence results of the biconjugate residual algorithm for solving generalized Sylvester matrix equation, Asian J. Control 19 (3) (2017) 961–968.

[34] M. Hajarian, Finite algorithms for solving the coupled Sylvester-conjugate matrix equations over reflexive and Hermitian reflexive matrices, Int. J. Syst. Sci. 46 (3) (2015) 488–502.

[35] Y. Zhang and S. S. Ge, Design and analysis of a general recurrent neural network model for time-varying matrix inversion, IEEE Trans. Neural Networks 16 (6) (2005) 1477–1490.

[36] D. Fu, H. Wang, X. Xiao, S. Liao, and L. Jin, Adaptive zeroing-gradient controller for ship course tracking with near singularity considered and zero theoretical tracking error, IEEE Access 7 (2019) 38205–38212.

[37] Y. Qi, L. Jin, H. Li, Y. Li, and M. Liu, Discrete computational neural dynamics models for solving time-dependent Sylvester equations with

applications to robotics and MIMO systems, IEEE Trans. Ind. Inf. In Press DOI 10.1109/TII.2020.2966544

[38] R. A. Horn and C. R. Johnson, Matrix Analysis, Cambridge Univ. Press., Cambridge, 2012.

[39] D. Guo and Y. Zhang, Zhang neural network for online solution of time-varying linear matrix inequality aided with an equality conversion, IEEE Trans. Neural Networks Learn. Sys. 25 (2) (2014) 370–382.

[40] A. V. Oppenheim and A. S. Willsky, Signals and Systems, Prentice-Hall, New Jersey, 1997.

[41] J. H. Mathews and K. D. Fink, Numerical Methods Using MATLAB, fourth ed., Prentice Hall, New Jersey, 2004.

[42] Y. Shi and Y. Zhang, New discrete-time models of zeroing neural network solving systems of time-variant linear and nonlinear inequalities, IEEE Trans. Syst. Man. Cybern. Syst. 50 (2) (2020) 565–576.